

# RSC Advances



This is an *Accepted Manuscript*, which has been through the Royal Society of Chemistry peer review process and has been accepted for publication.

*Accepted Manuscripts* are published online shortly after acceptance, before technical editing, formatting and proof reading. Using this free service, authors can make their results available to the community, in citable form, before we publish the edited article. This *Accepted Manuscript* will be replaced by the edited, formatted and paginated article as soon as this is available.

You can find more information about *Accepted Manuscripts* in the [Information for Authors](#).

Please note that technical editing may introduce minor changes to the text and/or graphics, which may alter content. The journal's standard [Terms & Conditions](#) and the [Ethical guidelines](#) still apply. In no event shall the Royal Society of Chemistry be held responsible for any errors or omissions in this *Accepted Manuscript* or any consequences arising from the use of any information it contains.

Cite this: DOI: 10.1039/c0xx00000x

ARTICLE TYPE

www.rsc.org/xxxxxx

## A facile approach to transform stainless steel mesh into pH-responsive smart material

Fuchao Yang <sup>a,c</sup> and Zhiguang Guo <sup>\*a,b</sup>*Received (in XXX, XXX) Xth XXXXXXXXX 20XX, Accepted Xth XXXXXXXXX 20XX*

DOI: 10.1039/b000000x

The mixed modifiers of methyl-terminated thiol and carboxyl-terminated thiol were successfully assembled on stainless steel meshes (SSM) utilizing polydopamine as adhesion layer and the strong thiol ligand with Ag. The microstructure, surface topography, chemical composition and wettabilities were investigated with X-ray diffraction (XRD), field emission scanning electron microscopy (FESEM), X-ray photoelectron spectroscopy (XPS) and contact angle meter, respectively. Importantly, the surface modified by mixed thiol show different responsive behavior to nonbasic and basic water droplets. Plus, the selectiveness of high water/oil repellence reveals the unique and smart of as-prepared functional stainless steel mesh. The reversible pH-response and stability have also been investigated. Based on stainless steel material widely used in engineering, this prepared smart material is expected to be used in many industrial applications, such as pH controllable dual oil/water on-off switch, diversified oil/water separation.

### Introduction

Driven by the desperation to develop technologically intelligent materials, much attention has long been focused on the smart surfaces that can show switchable and reversible water/oil wettability under external stimuli such as pH/solvent environmental changes, heat treatment, mechanical stress, light irradiation and applied electrical potential.<sup>1-3</sup> Among these external stimuli species, pH-responsive wettable material is important because it not only has many advantages, such as easy operation, quick responsiveness but also has wide applications in smart bioactive surfaces, drug or gene delivery and molecular recognition agents.<sup>4,5</sup> Leblond et al have reported a pH-sensitive molecular tweezer prototype that could serve as a fast responding unit to manipulate the release rate of a substrate (quinizarin) by a macromolecular carrier.<sup>6</sup> We have reported the pH-responsive porous material with designed wettability can be applied to separate an oil-and-water mixture bidirectionally.<sup>7</sup> Lee et al have reported electrospun poly(DPAEMA-co-TSPM)-coated fabrics with a pH-responsive tunable wettability that alternated between superhydrophobic in a basic solution and superhydrophilic in an acidic solution.<sup>8</sup> The retiform substance is good for saving raw material and is born with the function of filtration. Not only that, stainless steel meshes (SSM) also possess the properties of strong mechanic strength and can be cheap available. It has broad applications in engineering field and daily life. So the transformation of SSM into pH-responsive smart material can draw considerable attention in our view.

Cao and Feng et al have successfully fabricated the thermo and

pH dual-controllable oil/water separation materials based on SSM by photo initiated free radical polymerization of dimethylamino ethyl methacrylate.<sup>9</sup> They carried out Cu electrodeposition, and used dimethylamino ethyl methacrylate as monomer, N,N'-methylene bisacrylamide as the chemical cross-linker, and polyacrylamide as thickener under UV-light for polymerization. They employed poly (dimethylamino) ethyl methacrylate (PDMAEMA) as the thermo and pH dual-responsive functional group. An alternative and easy approach, our main idea is to graft pH-responsive thiol functional group on the SSM with enhanced rough Ag layer by being deposited in situ and self-assembly method of modification afterwards. Methyl-terminated thiol is low surface energy materials without stimulus-response property and carboxyl-terminated thiol is pH-responsive without hydrophobic property.<sup>10,11</sup> Amalric et al have investigated the potential of phosphonate self-assembled monolayers functionalized by silver thiolate species as antibacterial nanocoatings for inorganic biomaterials.<sup>12</sup> Ag is also chosen by us to increase the roughness of SSM surface because it is an ideal candidate for corrosion resistant, anti-bacterium and can also form stable coordination complexes with thiol.<sup>12, 13</sup> However, how to anchor Ag particles on SSM surface is a question indeed. Mussel-inspired polydopamine (PDA) was found to have the enormous power of adhesion to almost all kinds of surfaces (highly stronger than adsorption on fabrics) because of the catechol motif.<sup>14</sup> The broad applications of PDA were also highlighted by the much mild solution oxidation method of self-polymerization reaction. Lee et al reported the deposition of Ag via simple dip-coating of PDA-coated objects into silver nitrate

solution.<sup>15</sup> We have reported the PDA layer as strong adhesive for Ag<sub>2</sub>O nanoparticles possessing the ability of good wear resistance.<sup>16</sup>

Combining with the advantages of above materials, herein we develop a synergetic strategy and the facile synthesis of pH-responsive behavior of smart interface based on SSM. The aim of this study is to deliver a reference for resolving key issues of developing smart interfacial materials and devices.

## Materials and methods

### Materials

SSM with about 400 meshes per square inch is commercially available and tailored into the size about 4.0 cm × 4.0 cm. 3-hydroxytyramine hydrochloride (dopamine hydrochloride, 99.5%), tris(hydroxymethyl) aminomethane (99.5%, coded as Tris), n-Decyl thiol (HS(CH<sub>2</sub>)<sub>9</sub>CH<sub>3</sub>) and 11-mercaptopundecanoic acid (HS(CH<sub>2</sub>)<sub>10</sub>COOH) were purchased from Sigma-Aldrich. Silver nitrate (AgNO<sub>3</sub>) was obtained from Sinopharm Chemical Reagent Co., Ltd., P. R. China. All of the chemicals were analytical-grade reagents and used as received. The acidic aqueous phase at pH = 1 was prepared by dissolving hydrochloric acid at preassigned concentrations. The basic aqueous phases at pH = 13.5 were prepared by dissolving KOH in deionized water at preassigned concentrations. The label number of used gasoline in experiment is 93#.

### Fabrication of functional stainless steel mesh

The raw SSM were sequentially cleaned with deionized water, anhydrous ethanol, and deionized water in an ultrasonic cleaner for 10 min to remove possible impurities. The cleaned SSM were immersed in Tris-HCl solution (10mM, 15ml) of dopamine (0.03 g) for 12 h, cleaned by ethanol and ultrapure water in turns, and dried under nitrogen flow to finish self-polymerization of dopamine. The thickness of PDA film on SSM surface was about 40–50 nm.<sup>14,15,17</sup> The processed SSM was immersed into 0.05 M AgNO<sub>3</sub> aqueous solution (20 ml) at room temperature and then 10 ml aqueous solution of 0.05 M ascorbic acid (C<sub>6</sub>H<sub>8</sub>O<sub>6</sub>) was added dropwise into the solution under vigorous stirring for half an hour. Mechanical stirring device was used to avoid the influence of magneton. After fabrication of Ag, different cleaned and dried SSM were immersed separately into the n-Decyl thiol ethanol solution (1 mM 20 ml) and the 20 ml mixed thiol ethanol solution (n-Decyl thiol and 11-mercaptopundecanoic acid) for 12 h. The mixed thiol concentration ratio of HS(CH<sub>2</sub>)<sub>9</sub>CH<sub>3</sub> and HS(CH<sub>2</sub>)<sub>10</sub>COOH was 1:1 and the total concentration of the thiol in ethanol solution was 1 mM. After finishing the modification, the samples were then thoroughly cleaned several times with anhydrous ethanol to remove any residual thiol, followed by drying in a drying oven.

### Characterization.

The crystal structures of the as-prepared samples were characterized by X-ray diffraction (XRD) using a X'PERT PRO diffractometer with Cu K $\alpha$  radiation of 1.5418 Å wavelength at 2 $\theta$  ranging from 20° to 90°. Scanning electron microscopy (SEM) images were obtained on JEOL JSM-5600LV and field emission scanning electron microscope (FESEM) images were obtained on JSM-6701F both with Au-sputtered specimens. X-

ray photoelectron spectroscopy (XPS, PANalytical MagixPW 2403) measurement using the Al K $\alpha$  line as the excitation source was carried out for the examination of the chemical composition of the as-prepared SSM. The elements present in the sample surface were identified from a survey spectrum recorded over the energy range 0–1200 eV at a interval of 1 eV. High resolution (0.1 eV) spectra were then recorded for pertinent photoelectron peaks to identify the chemical state of a specified element. All the binding energies were referenced to the C1s neutral carbon peak at 284.8 eV, to compensate for the effect of surface charging. The water contact angles (CA) were measured with a DSA100 contact angle meter (Kruss Company, Germany) or JC2000D with a 5  $\mu$ L distilled water droplet at ambient temperature. The sliding angles (SA) were measured by DSA100 contact angle meter. The average CA and SA values were obtained by measuring the same sample at several different positions. The optical photographs and videos were captured with a traditional digital camera: DSC-HX200 camera and Olympus optical microscope (BX51).

## Results and discussion

Figure 1 exhibits wide angle XRD patterns of the pristine and different modified surface on SSM. The characteristic peaks marked with ■ are attributed to the SSM substrate whereas the characteristic peaks marked with ● are attributed to the as-deposited Ag particles. Sample (a), (b), (c), (d) and (e) are corresponding to original SSM, polymerization of dopamine, adhesion of Ag particles, modification of methyl-terminated thiol and mixed thiol on SSM surface, respectively. In Fig. 1, the diffraction peaks from neat SSM at 43.58°, 50.73° and 74.63° can be attributed to (111), (200) and (220) of austenitic steel (JCPDS no. 033-0945). The diffraction peaks at 38.18°, 44.35°, 64.50°, 77.49° and 81.56° are indexed to the (111), (200), (220), (311) and (222) planes of face-centered cubic silver (JCPDS No. 04-783).<sup>18</sup> No other crystalline phases of Ag were detected. By comparison, the XRD pattern of (b) is very similar to that of (a), indicating that PDA has no big effect on the crystal structures of SSM. The XRD spectra of (d, e) are also similar to that of (c).

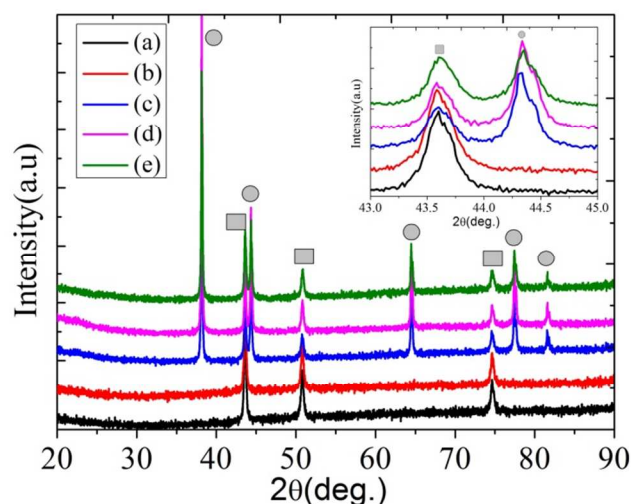
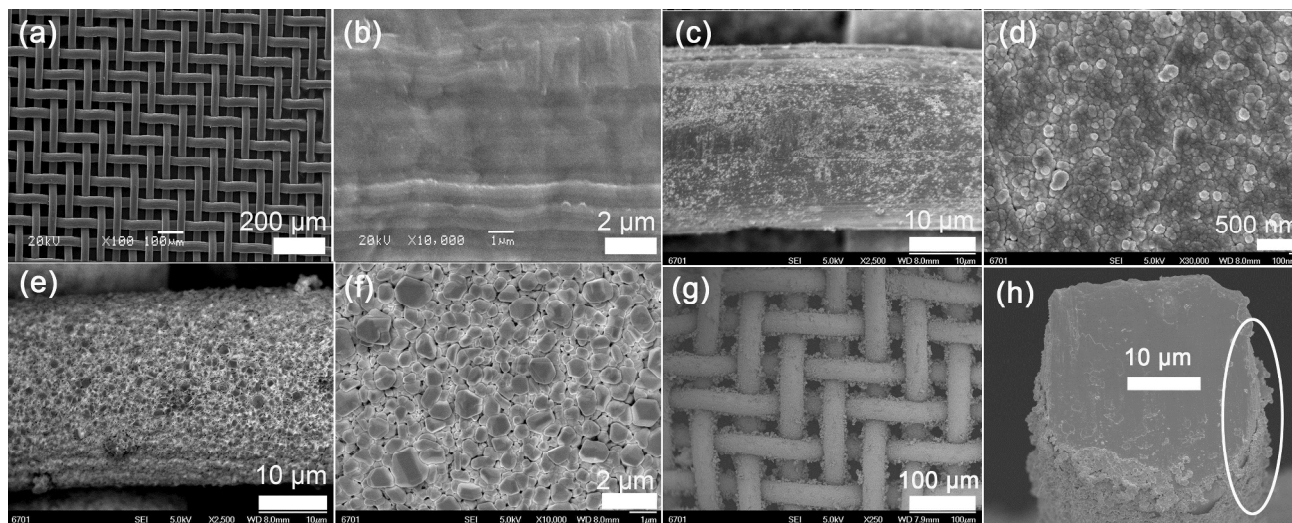


Fig. 1 XRD patterns of pristine (a), PDA modified (b), Ag modified (c), methyl-terminated thiol modified (d), and mixed thiol modified (e) surface on SSM.

The inset gives the enlarge view of 2θ position at 43-45° showing (200)



**Fig. 2.** SEM morphologies of pristine SSM: (a) and (b). FESEM morphologies of PDA modified the SSM surface (c and d), Ag particles modified the SSM surface (e and f). The holistic plan view (g) and cross-section view for a single wire (h) of mixed thiol modified SSM.

the small changes after each process. This detail indicates the diffraction peak of Ag would shift to a higher angle after thiol modification. Levard et al reported that the XRD patterns of synthetic Ag nanoparticles showed the presence of an additional phase after reaction with aqueous  $\text{Na}_2\text{S}$ .<sup>19</sup> Both results indicate that the XRD is sensitive to the presence of crystalline phases to Ag after sulfidation. Moreover, XPS was employed for detecting and confirming the Ag and other elements shown later in this paper.

Fig. 2a-b show the SEM images of pristine SSM. The meshes are well-distributed with the average diameter of about 40  $\mu\text{m}$  (Fig. 2a). It is clear that the surface of single wire is not smooth and the processed moulage is residual (Fig. 2b). The SEM images of several pores (or single pore), energy dispersive spectrometer and elements contents of SSM can be found in Fig. S1, 2 and Table S1 (ESI<sup>†</sup>). Fig. 2c-d shows the images of SSM surface modified by PDA, which was mainly composed of uniform and dense nanoparticles with grains size of about 100 nm. This surface is relatively flat. However it is disadvantageous for obtaining high water repellent property. As shown in Fig. 2e-f, after Ag particles deposition on stainless steel wires, the surface became concave-convex and turned to rough. This will enhance the wettability since high rough structure can magnify the hydrophobicity or hydrophilicity to extreme.<sup>20</sup> To acquire the high water/oil repellent surface, the thiol monomolecular layer was self-assembled on Ag surface. Meanwhile, the morphology has no obvious change after thiol modification and details of its magnification can be seen in Fig. S3 (ESI<sup>†</sup>). It can be seen in Fig. 2g that the pore channels indeed exist after multistep modifications. Fig. 2h presents the cross-section view for a single wire of the final smart SSM, indicating the thickness of Ag layer is about 0.4  $\mu\text{m}$ .

To further confirm the co-existence of PDA, Ag and thiol in these samples, XPS has been performed. As shown in Fig. 3(i), it can be clearly observed that the C1s peak is quite high for pristine SSM while the dominant peak for n-Decyl thiol (or mixed thiol) modified SSM is the Ag 3d. The N element signal arised from

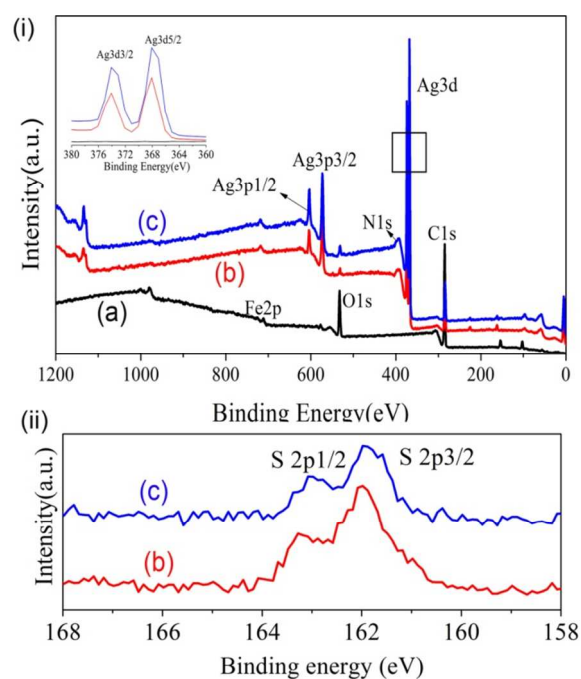


**Fig.3** (i) XPS survey analysis of (a) original SSM, (b) n-Decyl thiol and (c) mixed thiol modified SSM surface (ii) High-resolution spectra of S2p

PDA can be found at the binding energy of 396.1 eV for N1s.<sup>21</sup> The peaks of Ag element arising from the deposition of Ag particles are observed at the binding energy of several values. For Ag 3p, two peaks are observed at binding energies of about 604.1 and 572.1 eV, corresponding to Ag 3p<sub>1/2</sub> and Ag 3p<sub>3/2</sub>.<sup>21</sup> For Ag 3d, the indicated rectangular region was magnified and given as inset figure. The two peaks are observed at binding energies of about 374.1 and 368.1 eV, corresponding to Ag 3d<sub>3/2</sub> and Ag 3d<sub>5/2</sub>.<sup>21,22</sup> The S element corresponding to the n-Decyl thiol or 11-mercaptoundecanoic acid has also been detected and its high-resolution spectra has been given in Fig. 3(ii). The S2p<sub>1/2</sub> and

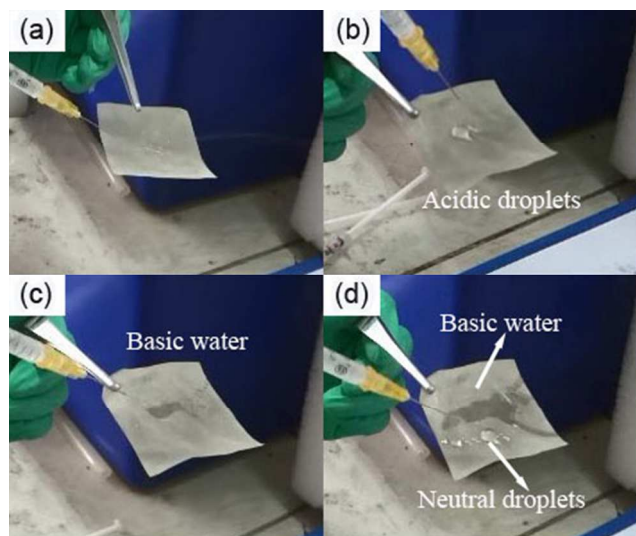


**Fig.4** (a) Neutral water on SSM modified by n-Decyl thiol. (b) Acidic water droplets on SSM modified by mixed thiol. (c) Basic water droplets on SSM modified by mixed thiol. (d) Basic and neutral water droplets on SSM modified by mixed thiol

$2p_{3/2}$  peaks, located at 163.2 eV and 162.0 eV with slightly decrease in contrast to free alkanethiol (163.5~163.8 eV), indicating that the alkanethiols or mercaptoundecanoic acid are chemisorbed via the  $-SH$  group and the alkanethiols or 11-mercaptoundecanoic acid are packed density on Ag surface (S-Ag bond forms) in the modification process.<sup>23</sup>

Some intuitionistic and interesting experimental phenomena can be found and then described as follows. If the SSM surface modified by methyl-terminated thiol is inclined more than about 15°, acidic droplets, neutral droplets and basic droplets would roll off and have no evident differences. If acidic, neutral or basic water column squirted on a piece of SSM modified by methyl-terminated thiol, the impacting water column would bounce out of this surface, exhibiting extremely similar phenomenon. And the case of neutral water was given in Fig.4a as the representative of other similar situations. As shown in Fig.4b, acidic water droplets show quasi-spherical shape on mixed thiol modified SSM surface. The quasi-spherical shape implies a high lyophobic surface for these acidic droplets. In Fig.4c, when the water droplets are basic, it can not stand with any shape and would penetrate into the meshes. So the plain SSM is transformed into pH-responsive smart material, exhibiting quite different behaviors when it encounters acidity or alkali. Mierczynska et al pointed out that the pH responsive change in the slope of the wettability gradient might be useful in moving liquids across surfaces.<sup>24</sup> For clear observation and comparison, the neutral water droplets was dripped aside the basic wetted zone of the same sample and exhibited sphericity, shown in Fig.4d. The differences between neutral and alkaline water droplets on SSM surface modified by mixed thiol are remarkable while the distinction between acidic and neutral water droplets on the same surface are beyond distinguishing without the help of instrument. Next, the DSA100 contact angle meter is employed.

To quantitative evaluation the wettability behavior of different modified SSM surface, the measurement of the CA by the 'sessile drop' method was conducted. In Fig.5a, CAs of sample (1), (2),

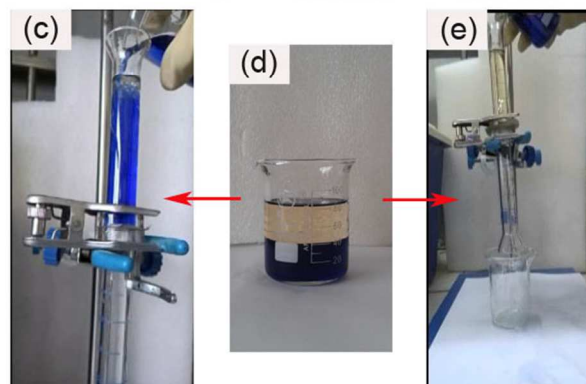
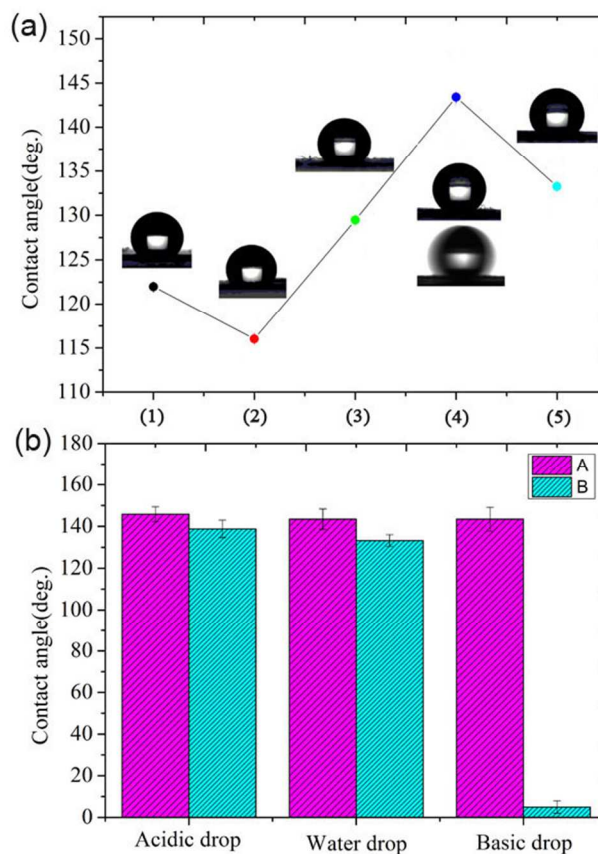


**Fig. 5** (a): Wettability of water droplets on pristine and different modified SSM surface. (b): Wettability of acidic droplets, neutral droplets and basic droplets on SSM modified by methyl-terminated thiol (A) and mixed thiol (B). (c): High water repellence of the SSM modified by mixed thiol. (d): The mixture of petrol and water. (e): High oil repellence of the SSM modified by mixed thiol and pre-wetted by alkaline solution.

(3), (4) and (5) are corresponding to 5  $\mu$ L deionized water droplet on surface of original SSM (121.9°), polymerization of dopamine (116.0°), adhesion of Ag particles (129.5°), modification of methyl-terminated thiol (143.4°) and mixed thiol (133.2°). A noteworthy feature of SSM modified by PDA is that its colour changed from off-white to brown, water droplets on its surface was unstable, and the shape became rectangle finally (Fig. S4, ESI†). The sliding angle of SSM surface modified by methyl-terminated thiol, which is the inclination angle of the surface from which the deionized water droplet can roll off, is about 13° (inset of Fig.5a). As Fig.5b shown, on the SSM surface modified

by methyl-terminated thiol, the CA of acidic droplets, neutral droplets and basic droplets have no significant differences with centering at about 143°. Whereas the CA of acidic droplets, neutral droplets and basic droplets on the SSM surface modified by mixed thiol are 138.8°, 133.2° and less than 5°. The modified meshes treated with non-alkaline and alkaline water in a quite different behavior: high hydrophobicity for acidic or neutral water droplets while superhydrophilicity for alkaline water droplet. This result confirmed that as-prepared SSM provides the pH-responsive effect. The as-prepared smart meshes have the advanced selective permeability not only to non-alkaline and alkaline water but also to deionized water and oil. In Fig.5d, the deionized water was dyed with methylene for clear observation. The functional SSM possessed high water repellence and can be used for oil-water separation (Fig.5c). The separation efficiency of oil/water mixture is defined by the ratio between the weight of oil (gasoline) collected and that the initially added to the mixture. The average separation efficiency based on five recycles is calculated to be 90.6% (Fig.S5, ESI†). However, if the as-obtained SSM was immersed in basic solution for about 5 minutes, the smart SSM become extremely hydrophilic and high oil repellent after being pre-wetted as shown in Fig.5e. As it is widely accepted that, hydrophilic surface often possess high oil repellent when they trapped water or underwater surrounding. The intrusion pressure of water (or oil), which indicates the maximum height of water (or oil) that the as-obtained meshes can support, can be calculated by the following equation:<sup>26</sup>

$$P = \rho_{liq} g h_{max} \quad (1)$$

where  $P$  is the intrusion pressure.  $\rho_{liq}$  is the density of water ( $1.0 \times 10^3 \text{ kg/m}^3$ ) or oil ( $0.71 \times 10^3 \text{ kg/m}^3$ ).  $g$  is acceleration of gravity ( $9.80 \text{ m/s}^2$ ), and  $h_{max}$  is the maximum height of water (9.52 cm) or oil (8.70 cm) that the mixed thiol modified SSM mesh can support. The results of calculation indicate that the intrusion pressure is about 932.96 Pa for water (605.35 Pa for oil).

With the development of smart devices, reversibly controlling the surface wettability has aroused great interest.<sup>27-29</sup> Interestingly, this smart meshes show reversible transition between the high hydrophobicity and superhydrophilicity after being immersed into the acidic (pH = 1) or alkaline (pH = 13.5) solution for 5 minutes and being dried under nitrogen. The variation of CAs are between about 130° (after acidic soak) and close to 0° (after alkaline soak). This process can be repeated several times and shows good recyclability, as shown in Fig.6a. The corresponding mechanism is discussed later in this paper. Bird et al have reported biodegradable pH-responsive hollow polymer particles. They demonstrated the pH-triggered swelling of the hollow particles and pH-triggered release of a model solute from the new hollow particles.<sup>30</sup> The reversible pH-responsive material can offer excellent potential for future application in smart device.

The stability of smart SSM can also be proven by the abrasion test and high temperature durable test followed.<sup>31</sup> Sandpaper (1500 mesh) served as an abrasive surface to test the mechanical stability of as-prepared SSM. The sample was subjected to a 200 g weight and was kept in close contact with the sandpaper. The modified SSM was then moved slowly back and forth with a speed of about 2 cm/s and an abrasion length of 20 cm.<sup>32-33</sup> As

shown in Fig.6b, the ability of hydrophobicity was partially lost after 15 cycles of abrasion test. However, our samples possessed

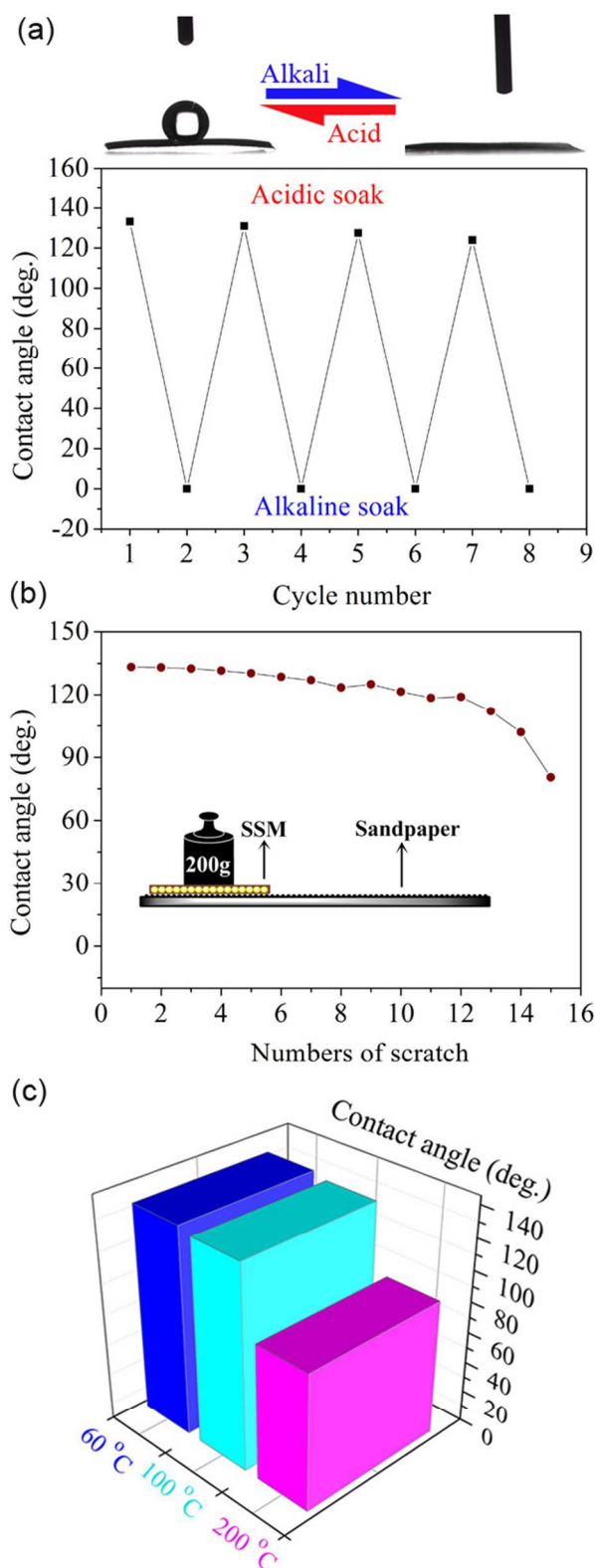


**Fig.6** (a) Reversible transition between the high hydrophobicity and superhydrophilicity (b) The variation of water CAs on SSM surface scratched by the sandpaper (c) The water CA on SSM surface endured different high temperatures

a relative high level of hydrophobicity within 10 cycles, indicating a certain degree of durability against abrasion. The thermal stability was studied via an investigation of water droplets on the as-prepared SSM surface subjected to different

Table 1 Solubility product constant of different transition-metal sulfides

| Ag <sub>2</sub> S | ZnS (α) | CuS | NiS | CoS (α) | FeS |
|-------------------|---------|-----|-----|---------|-----|
|-------------------|---------|-----|-----|---------|-----|

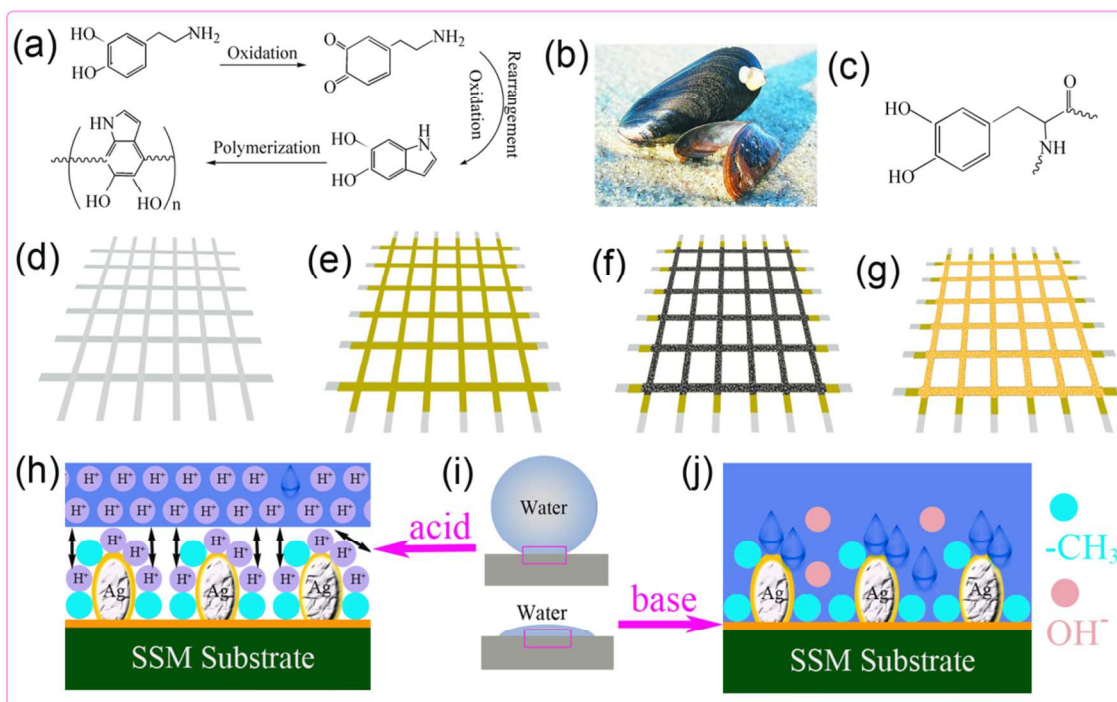


**Fig. 7** The self-polymerize of PDA (a), photo of mussels (b), structure of DOPA (c). Schematic diagram for the preparation process (d-g) and formation mechanism (h-j) of smart SSM.

5 temperatures. As shown in Fig. 6c, the CAs of water droplets on the as-prepared SSM surface subjected to 60 °C for 10 h and 100 °C for 10 h was nearly unchanged, larger than 130°. This results indicate that the smart SSM surface shows good stability under high temperature condition. However, when the temperature was

10 further raised up, the CAs of water droplets on the treated SSM decreased to 87.5° even though the duration was shortened to 5h.

Finally, the formation and response mechanism of the smart SSM are also discussed. Dopamine can be oxidized and spontaneously polymerized under mild conditions (Fig. 7a). 3,4-dihydroxy-*L*-phenylalanine (DOPA) is believed to contribute to extraordinarily robust adhesion, by which mussels (Fig. 7b) can achieve long-lasting adhesion and strongly attach to all kinds of substrates, even on wet surfaces.<sup>14,34</sup> Dopamine is structurally mimic of DOPA (Fig. 7c). Taking the well-being of self-

20 polymerized dopamine, the fabrication sequence involved three steps. In the first step, the cleaned SSM (Fig. 7d) was chosen as substrate for PDA deposition. Next, the SSM packed by PDA (Fig. 7e) is used to anchoring Ag particles on SSM (Fig. 7f). Here the Ag particles serves two purposes: it provides a rough structure

25 for enhanced wettability and it also sets the methyl-terminated thiol and carboxyl-terminated thiol, which in this case is stable and robust.<sup>35</sup> In the last step, the functional groups of *n*-Decyl thiol or mixed thiol were self-assembled on the SSM substrate (Fig. 7g). Ag has much lower solubility product constant ( $K_{sp}$ )

30 with sulfur than many other common transition-metals as shown in Table 1.

|           |                       |                       |                       |                       |                       |                       |
|-----------|-----------------------|-----------------------|-----------------------|-----------------------|-----------------------|-----------------------|
| $K_{sp}$  | $6.3 \times 10^{-50}$ | $1.6 \times 10^{-24}$ | $6.3 \times 10^{-36}$ | $2.0 \times 10^{-26}$ | $4.0 \times 10^{-21}$ | $6.3 \times 10^{-18}$ |
| $pK_{sp}$ | 49.20                 | 23.80                 | 35.20                 | 25.7                  | 20.40                 | 17.2                  |

The values given in the above table were cited from Lange's Chemistry Handbook, 15th Edition.

35 Solubility product constant ( $K_{sp}$ ) is a constant that here reflects the strength of transition-metal and sulfide ligand interactions. The solubility product behavior indicates that the low value levels are associated with high ligand interactions. The  $pK_{sp}$  given in Table 1 is only another form of  $K_{sp}$  after mathematical operation.

40 This low  $K_{sp}$  constant (or high  $pK_{sp}$ ) also indicates the formation of sulfide nucleation is abundant, and so the generated sulfide has strong interest in growing on the Ag surface.<sup>36</sup> The strong bonding effects between thiol and Ag surface is a prerequisite for achieving high hydrophobic and smart surface. The outcome of

45 pH-response can be understood by the protonation and deprotonation effects of carboxylic acid groups grafted on the SSM surface (Fig.7h, i and j). When the acidic water droplets contacted the mixed thiol modified surface, the plentiful  $H^+$  of acidic liquid triggers  $H^+$  ionic repulsive interactions with

50 carboxylic acid groups (Fig.7h). The acceptance of protons in 11-mercaptoundecanoic acid leads to extending of the molecules chain of alkyl groups, which are induced by the electrostatic repulsion of the generated charges.<sup>37</sup> Together with the help from physical crosslink with *n*-Decyl thiol (hydrophobic groups) and

55 architectural rough surface generated by Ag particles, so the surface is extremely repellent to acidic water droplet. When

neutral water droplets contacted the mixed thiol modified surface, the main difference from above situation is that the existence of H<sup>+</sup> ionic repulsive interactions was localized only between the molecules of the 11-mercaptoundecanoic acid. As for basic water droplet contacted the mixed thiol modified surface, the abundant OH<sup>-</sup> of basic water droplets would wipe out the H<sup>+</sup> of carboxylic acid groups. The release of protons in 11-mercaptoundecanoic acid leads to collapsing of the molecules chain of alkyl groups. Along with the physical crosslink with n-Decyl thiol and amplification of Ag rough surface, so the mixed thiol modified surface is superhydrophilic to basic water droplets. That's the reason why these smart meshes treated with non-alkaline and alkaline water in quite different behaviors.

## Conclusions

In conclusion, we report a simple solution-based method for the preparation of n-Decyl thiol and mixed thiol (n-Decyl thiol and 11-mercaptoundecanoic acid) modified SSM surface. The SSM surfaces modified by methyl-terminated thiol are extremely water repellent and the CA of acidic droplets, neutral droplets and basic droplets have no significant differences with centering at about 143°. The SSM surface modified by mixed thiol is transformed into pH-responsive smart material, exhibiting quite different behavior when it encounters acidity or alkali. The CA of acidic droplets, neutral droplets and basic droplets on this surface are about 138.8°, 133.2° and less than 5°. This smart meshes exhibit the advanced selective permeability not only to non-alkaline and alkaline water but also to deionized water and oil. Reversible transition between high hydrophobicity and superhydrophilicity can be achieved after being treated by acid or alkali. The CAs of water droplets on the as-prepared SSM surface were nearly unchanged after being subjected to abrasion test within 10 cycles and high temperature at 100 °C for 10 h. The mechanism is dependent on the acceptance or release of protons of carboxyl-terminated thiol leading to extending or collapsing of the relative molecules chain. The synergetic effect of Ag rough surface also plays an important role in the final desirable results.

## Acknowledgements

This work is supported by the National Nature Science Foundation of China (Nos. 11172301 and 21203217), the "Funds for Distinguished Young Scientists" of Hubei Province (No. 2012FFA002), the "Western Light Talent Culture" Project, the Co-joint Project of Chinese Academy of Sciences, and the "Top Hundred Talents" Program of Chinese Academy of Sciences.

## Notes and references

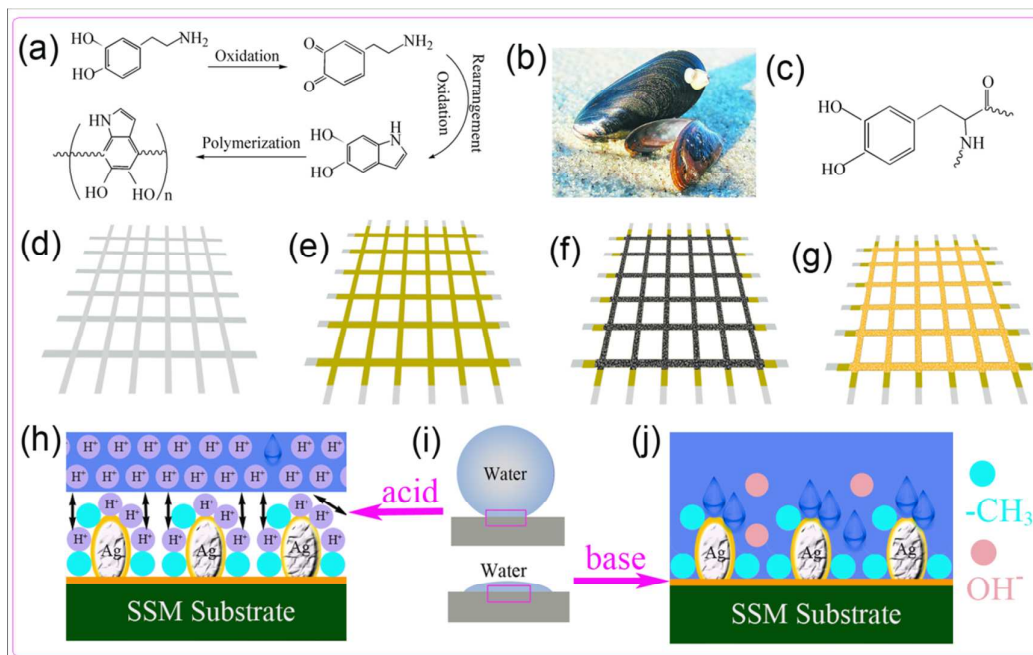
- <sup>a</sup> State Key Laboratory of Solid Lubrication, Lanzhou Institute of Chemical Physics, Chinese Academy of Sciences, Lanzhou 730000, People's Republic of China. Tel: 0086-931-4968105; Fax: 0086-931-8277088; Email: zguo@licp.cas.cn.  
<sup>b</sup> Hubei Collaborative Innovation Centre for Advanced Organic Chemical Materials and Ministry of Education Key Laboratory for the Green Preparation and Application of Functional Materials, Hubei University, Wuhan 430062, People's Republic of China  
<sup>c</sup> Graduate School of Chinese Academy of Sciences, Beijing 100049, People's Republic of China

† Electronic Supplementary Information (ESI) available: [The SEM images of several pores (or single pore), energy dispersive spectrometer and elements contents of SSM are given in FIG. S1, 2 and Table S1. FIG. S3. Different magnifications of FESEM images of Ag-coated SSM after mixed thiol modification. FIG. S4. Photographs of (a) water drop on original SSM, (b) water drop on SSM modified by PDA. Photographs of acidic droplet (c), neutral droplet (d) and basic droplet on SSM modified by n-octadecyl thiol. FIG. S5. The separation efficiency of the smart meshes in oil/water separation experiments under multiple recycles]. See DOI: 10.1039/b000000x/

- 1 R. Wang, K. Hashimoto, A. Fujishima, M. Chikuni, E. Kojima, A. Kitamura, M. Shimohigoshi and T. Watanabe, *Nature*, 1997, **388**, 431.
- 2 J. Lahann, S. Mitragotri, T.N. Tran, H. Kaido, J. Sundaram, I. S. Choi, S. Hoffer, G. A. Somorjai and R. Langer, *Science*, 2003, **299**, 371.
- 3 J. Yang, X.H. Men, X.H. Xu and X.T. Zhu, *Langmuir*, 2010, **26**, 10198.
- 4 J.C. Chen, M.Z. Liu, C.M. Gao, S.Y. Lu, X.Y. Zhang and Z. Liu, *RSC Adv.*, 2013, **3**, 15085.
- 5 Y. Liu, J.B. Li, J. Ren, C. Lin and J.Z. Leng, *Mater. Lett.*, 2014, **127**, 8.
- 6 J. Leblond, H. Gao, A. Petitjean, J.C.Leroux, *J. Am. Chem. Soc.*, 2010, **132**, 8544.
- 7 (a) B. Wang and Z.G. Guo, *Chem. Commun.*, 2013, **49**, 9416. (b) B. Wang, W. X. Liang, Z. G. Guo, W. M. Liu. *Chem. Soc. Rev.* 2015, **44**, 336.
- 8 C. H. Lee, S. K. Kang, J. A. Lim, H. S. Lim and J. H. Cho, *Soft Matter*, 2012, **8**, 10238.
- 9 Y.Z. Cao, N. Liu, C.K. Fu, K. Li, L. Tao, L. Feng and Y. Wei, *ACS Appl. Mater. Interfaces*, 2014, **6**, 2026.
- 10 M.J. Cheng, Q. Liu, G.N. Ju, Y.J. Zhang, L. Jiang and F. Shi, *Adv. Mater.*, 2014, **26**, 306.
- 11 Y.L. Zhang, X.G. Kong, B. Xue, Q.H. Zeng, X.M. Liu, L.P. Tu, K. Liu and H. Zhang, *J Mater. Chem. C*, 2013, **1**, 6355.
- 12 J. Amalric, P. H. Mutin, G. Guerrero, A. Ponche, A. Sottoc and J.-P. Lavigne, *J. Mater. Chem.*, 2009, **19**, 141.
- 13 J. Li, L. Shi, Y. Chen, Y. B. Zhang, Z. G. Guo, B.L. Su and W. M. Liu, *J. Mater. Chem.*, 2012, **22**, 9774.
- 14 Y.L. Liu, K.L. Ai and L.H. Lu, *Chem. Rev.*, 2014, **114**, 5057.
- 15 H. Lee, S.M. Dellatore, W.M. Miller and P. B. Messersmith, *Science*, 2007, **318**, 426.
- 16 S.F. E, L. Shi and Z.G. Guo, *RSC Adv.*, 2014, **4**, 948.
- 17 F. Bernsmann, V. Ball, F. Addiego, A. Ponche, M. Michel, J. J. de Almeida Gracio, V. Toniazio, D. Ruch, *Langmuir*, 2011, **27**, 2819.
- 18 Y.J. Zhuo, W.D. Sun, L.H. Dong and Y. Chu, *Appl. Surf. Sci.*, 2011, **257**, 10395.
- 19 C. Levard, B. C. Reinsch, F. M. Michel, C. Oumahi, G. V. Lowry and G. E. Brown Jr, *Environ. Sci. Technol.*, 2011, **45**, 5260.
- 20 K.Q. Li, X.R. Zeng, H.Q. Li, X.J. Lai and H. Xie, *Mater. Lett.*, 2014, **2**, 255.
- 21 C.D. Wagner, W.M. Riggs, L.E. Davis and J.F. Moulder, *Handbook of X-ray photoelectron spectroscopy*, 1979; A. V. Naumkin, A. Kraut-Vass, S. W. Gaarenstroom and C. J. Powell, *NIST X-ray Photoelectron Spectroscopy Database 20*, Version 4.1, 2012.
- 22 H.C. Yu, Q.S. Dong, Z.B. Jiao, T. Wang, J.T. Ma, G.X. Lu and Y.P. Bi, *J. Mater. Chem. A*, 2014, **2**, 1668.
- 23 T. P. Ang, T. S. A. Wee and W. S. Chin, *J. Phys. Chem. B*, 2004, **108**, 11001.
- 24 A. Mierczynska, A. Michelmor, A. Tripathi, R.V. Goreham, R. Sedev and K. Vasilev, *Soft Matter*, 2012, **8**, 8399.
- 25 N. Liu, Y.Z. Cao, X. Lin, Y.N. Chen, L. Feng and Y. Wei, *ACS Appl. Mater. Interfaces*, 2014, **6**, 12821.
- 26 Z.X. Xue, S.T. Wang, L. Lin, L. Chen, M.J. Liu, L. Feng and L. Jiang, *Adv. Mater.*, 2011, **23**, 4270.
- 27 X.J. Feng, L. Feng, M.H. Jin, J. Zhai, L. Jiang and D.B. Zhu, *J. Am. Chem. Soc.*, 2004, **126**, 62.
- 28 W.P. Wang, Z. Xie, Z.C. Lia and Z.J. Zhang, *RSC Adv.*, 2015, **5**, 4524.
- 29 B.W. Xin and J.C. Hao, *Chem.Soc.Rev.*, 2010, **39**, 769.
- 30 R. Bird, T. Freemont and Brian R. Saunders, *Soft Matter*, 2012, **8**, 1047.
- 31 X.Y. Zhou, Z.Z. Zhang, X.H. Xu, F. Guo, X.T. Zhu, X.H. Men and B. Ge, *ACS Appl. Mater. Interfaces*, 2013, **5**, 7208.
- 32 W.X. Liang and Z.G. Guo, *RSC Adv.*, 2013, **3**, 16469.



- 
- 33 L. Wu, J.P. Zhang, B.C. Li and A.Q. Wang, *J. Mater. Chem. B*, 2013,  
1, 4756.
- 34 L. Zhang, J.J. Wu, Y.X. Wang, Y.H. Long, N. Zhao, J. Xu, *J. Am.  
Chem. Soc.*, 2012, **134**, 9879.
- 5 35 X.T. Zhu, Z.Z. Zhang, J. Yang, X.H. Xu, X.H. Men and X.Y. Zhou, *J.  
Colloid Interface Sci.*, 2012, **380**, 182.
- 36 M.S. León-Velázquez, R. Irizarry and M.E. Castro-Rosario, *J. Phys.  
Chem. C* 2010, **114**, 5839.
- 10 37 J. Zhang, S.S. You, S.K. Yan, K. Müllen, W.T. Yang and M.Z. Yin,  
*Chem. Commun.*, 2014, **50**, 7511.



a facile method for preparation of smart pH-responsive interface based on stainless steel mesh.